Atom Indonesia Vol. 40 No. 2 (2014) 63 - 67

Electronic and Optical Properties of Aluminum Oxide Before and After Surface Reduction by Ar^+ Bombardment

D. Tahir[1*], H.J. Kang[2] and S. Tougaard[3]
[1]*Department of Physics, Hasanuddin University,Tamalanrea, Makassar 90245, Indonesia*
[2]*Department of Physics, Chungbuk National University, Cheongju, 361-763 Korea*
[3]*Department of Physics, Chemistry and Pharmacy, Southern Denmark University, DK-5230 Odense M. Denmark*

ARTICLE INFO

Article history:
Received 18 November 2013
Received in revised form 12 June 2014
Accepted 25 June 2014

Keywords:
Sapphire
REELS
Electronic Properties
Optical Properties

ABSTRACT

The electronic and optical properties of α-Al_2O_3 after induced by 3-keV Ar^+ sputtering have been studied quantitatively by use of reflection electron energy loss spectroscopy (REELS) spectra. The band gap values of α-Al_2O_3 was determined from the onset values of the energy loss spectrum to the background level of REELS spectra as a function of time Ar^+ bombardment. The bandgap changes from 8.4 eV before sputtering to 6.2 eV after 4 minutes of sputtering. The optical properties of α-Al_2O_3 thin films have been determined by comparing the experimental cross section obtained from reflection electron energy loss spectroscopy with the theoretical inelastic scattering cross section, deduced from the simulated energy loss function (ELF) by using QUEELS-ε(k)-REELS software. The peak assignments are based on ELF and compared with reported data on the electronic structure of α-Al_2O_3 obtained using different techniques. The results demonstrate that the electronic and optical properties before and after surface reduction will provide further understanding in the fundamental properties of α-Al_2O_3 which will be useful in the design, modeling and analysis of devices applications performance.

INTRODUCTION

Ion bombardment to solids influence their properties due to a wide series of both compositional and structural changes. Quantitative studies of electronic and optical structure induced by ion bombardment are very scarce. The study of the reduction in case for metal oxide to lower oxidation state (even to metal) and the creation of point defect by low-energy ion bombardment have been reported in many studies [1-4].

In particular case of Alumina (Al_2O_3) or sapphire is one of the most important ceramics materials with exceptional properties such as great hardness, chemical inertness, and high melting temperature. It has many industrials applications such as catalysis, coatings, microelectronics, composite materials, and advanced materials technology [5]. The large area of applications makes the information about the effect of low-energy ion bombardment of great interest. To get a clear insight into the electrical properties of alumina for large area applications, a better understanding for the electronic and optical properties is necessary.

In the present work, the bandgap and the optical properties of α-Al_2O_3 before and after surface reduction with Ar^+ bombardment were obtained from the experimental inelastic scattering cross section of reflection electron energy loss spectroscopy (REELS) spectra for primary electron energies of 0.5, 1.0, 1.5 and 2.0 keV. Theoretical inelastic scattering cross section evaluated on the basis of Drude-Lindhard oscillators and using QUEELS-ε(k, ω)-REELS software to carry out quantitative analysis of REELS spectra [6]. REELS is surface sensitive and the spectra carry information on the electronic structure of the material because the energy loss experienced by the incident electron depends on the electronic structure of the material. The spectra can easily be recorded over a wide energy-loss range. We determined the electronic and optical quantities that consistently describe all experiments quantitatively. We note that the validity and consistency of this method was extensively tested recently [7], and it has previously been successfully used to obtain the electronic and optical properties of ultrathin dielectrics [8,9,11],

*Corresponding author.
E-mail address: dtahir@fmipa.unhas.ac.id

semiconductors [9-13], polymers [14], metals and their oxides [15] and transparent oxide films [16,17].

EXPERIMENTAL METHODS

As-received α-Al_2O_3 crystals were characterized *in situ* (without exposure to air) before and after each ion Ar^+ treatment. These treatments were applied in the main chamber with controlling the base pressure at ~10^{-8} mbar. Ar^+ beam bombardment was done with a Penning-type ion gun (AG 10 from VG scientific). Ion beams of 3-keV kinetic energy were applied for the used periods of time (1, 2, 3, and 4 minutes). REELS spectra of the samples were measured using VG ESCAlab 210 instrument and recorded at a constant pass energy mode of 20 eV, a few minutes after each bombardment treatment. The incident and take-off angles from the surface normal were 55° and 0°, respectively. The primary electron energies were 0.5, 1.0, 1.5 and 2.0 keV for excitation in REELS measurement. The energy resolution, given by the full width at half maximum of the elastic peak of backscattered electrons, was about 0.8 eV and the energy loss range was measured up to 100 eV.

The bandgap values were estimated from the REELS experimental data. The difference in energy between the elastic peak and the edge jump of the loss structure can be taken as an estimate of the bandgap. The experimental inelastic cross section from REELS spectra is obtained from the QUASES-XS-REELS software [18]. The method corrects the REELS spectrum for multiply scattered electrons and determines an effective single-scattering cross section, K_{exp} ($\hbar\omega$) times the corresponding inelastic mean free path λ, in the form of λK_{exp}.

RESULTS AND DISCUSSION

Figure 1 shows the REELS spectra for α-Al_2O_3 as a function of time (as labeled) Ar^+ bombardment on the surface. The bandgaps of α-Al_2O_3 were determined from the onset of loss energy in REELS spectra are 8.5, 6.9, and 6.5 eV before sputtering and after 1, 2, and 4 minutes of Ar^+ bombardment, respectively. It was found that the bandgap of α-Al_2O_3 after sputtering with Ar^+ decrease with increasing the sputtering time, indicating that the stoichiometric form of surface α-Al_2O_3 changed due to the breaking of chemical bonds between aluminum and oxygen atoms. Some of the oxygen atoms are easily removed from the surface of α-Al_2O_3 due to the oxygen atoms being lighter than the aluminum atoms. The aluminum atoms became more dominant on the surface of α-Al_2O_3 after sputtering compared with the surface of α-Al_2O_3 without sputtering. The increasing fraction of the aluminum atoms on the surface of α-Al_2O_3 after sputtering caused the reduced bandgap as shown in the REELS spectra in Fig. 1. These bandgap values were used as input parameters for the quantitative analysis of REELS spectra using QUEELS-ε(*k, ω*)-REELS software [6].

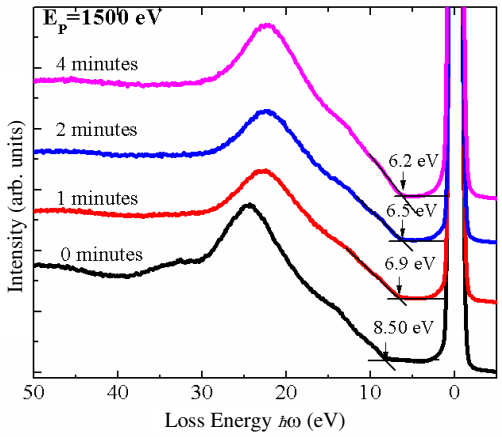

Fig. 1. Reflection energy spectra at energy 1.5 keV for α-Al_2O_3 as a function of sputtering times (as labeled).

The average theoretical electron inelastic scattering cross section $K_{th}(E_0, \hbar\omega)$ for all REELS electrons corresponding to a given REELS experiment can be calculated if the dielectric function is known. Here, E_0 is the primary electron energy and $\hbar\omega$ is the energy lost by an electron in a scattering event. In this software, all excitations are described by the dielectric function ε(*k*, $\hbar\omega$) of the material. The dielectric function gives the energy loss function (ELF) Im(-1/ε), which is parameterized as a sum of Drude-Lindhard type oscillators [6,7,19-21];

$$\mathrm{Im}\left[\frac{-1}{\varepsilon(k,\hbar\omega)}\right]=\sum_{i=1}^{n}\frac{A_i\gamma_i\hbar\omega}{((\hbar\omega_{0ik})^2-\hbar^2\omega^2)^2+\gamma_i^2\Delta E^2}x\theta(\hbar\omega-E_g) \quad (1)$$

with

$$\hbar\omega_{0ik}=\hbar\omega_{0i}+\alpha_i\frac{\hbar^2k^2}{2m} \quad (2)$$

where *Ai*, γ_I, $\hbar\omega$ and α_i are the oscillator strength, damping coefficient, excitation energy, and momentum dispersion coefficient of the i_{th} oscillator, respectively, and $\hbar k$ is the transferred momentum of electron from REELS to the solid.

The oscillator strength in ELF are adjusted to make sure by the well-established Kramers-Kronig sum rule [6,19-21],

$$\frac{2}{\pi}\int_0^\infty \mathrm{Im}\left\{\frac{1}{\varepsilon(\hbar\omega)}\right\}\frac{d(\hbar\omega)}{\hbar\omega} = 1-\frac{1}{n^2} \qquad (3)$$

where n is the refractive index in the static limit.

In Figure 2, as a standard reference to analysis, we show the comparison of the experimental inelastic cross section λK_{exp} (lines) and theoretical inelastic cross section λK_{th} (symbol) for α-Al_2O_3 thin films before and after sputtering. We used the QUEELS-XS-REELS software to obtain the experimental λK_{exp} derived from the raw experimental REELS spectra measured at 0.5, 1.0, 1.5 and 2.0 keV primary electron energies and QUEELS-$\varepsilon(k, \omega)$-REELS software to obtain theoretical inelastic cross section λK_{th}.

The parameters in the ELF were determined by trial and error procedure in which a test ELF function is adjusted until the agreement between the theoretical $K_{th}(E_0, \hbar\omega)$ and experimental inelastic cross section $K_{exp}(E_0, \hbar\omega)$ reproduces a successful fit. The successful fit (shown in Fig. 2) as a function of primary energy gives confidence in the validity of the model and thereby in the accuracy of the determined ELF. The theoretical inelastic cross sections were evaluated using the simulated ELF.

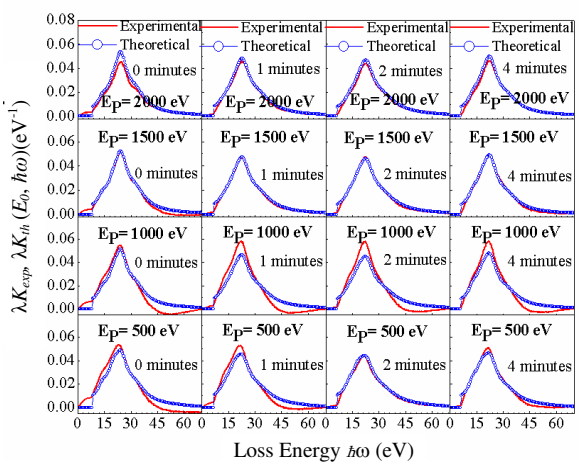

Fig. 2. Experimental inelastic cross section λK_{exp} for α-Al_2O_3 (red line) obtained from REELS data compared to theoretical inelastic cross sections λK_{th} (blue line) evaluated using the simulated energy loss function.

The parameters used to model ELF and surface energy loss function (SELF) for all materials considered are shown in Table 1. Those parameters were modified until the best overall agreement between the theoretical λK_{th} and the experimental λK_{exp} for all experiments was achieved. The ELF for α-Al_2O_3 used as input parameters for calculation of the theoretical cross-sections presented in Fig. 2 are depicted in Fig. 3. The spectra of ELF from Ref. [5] were obtained by analysis of valence electron energy loss spectroscopy (VEELS) spectra at primary electron energy at 100 keV for α-Al_2O_3. Those spectra are included as open circles in Fig. 3 for comparison. The observed peak for ELF of α-Al_2O_3 before sputtering has 3 oscillators in the vicinity of 15, 24.5 and 33 eV. These oscillators indicate that the loss energy peak position of electron traveling in the solid. The main feature in these spectra corresponds to the bulk plasmon peak at 24.5 eV for α-Al_2O_3 before sputtering, decreases slowly to 22.8 eV after sputtering for four minutes. The shift of the position of the bulk plasmon of α-Al_2O_3 after sputtering to the lower energies indicates that the stoichiometric form of α-Al_2O_3 changed after sputtering. We conclude that the electronic structure properties α-Al_2O_3 after sputtering with Ar^+ could change due to the decreasing quantity of oxygen in the compound.

Table 1. Parameters used to model energy loss functions of α-Al_2O_3 as a function of sputtering times according to Drude – Lindhard oscillator theory to give the best fit overall of experimental cross section

	i	$\hbar\omega_{0i}$ (eV)	A_i (eV^2)	γ_i (eV)
Al_2O_3 (0 minutes)	1	15.0	12.1	6.5
(E_g~8.5)	2	24.5	294.1	7.7
(α_i~0)	3	33.0	190.8	12
Al_2O_3 (1 minutes)	1	15.0	10.1	9.0
(E_g~6.9)	2	23.2	272.7	9.0
(α_i~0)	3	33.0	186.9	15.5
Al_2O_3 (2 minutes)	1	14.0	3.8	5.0
(E_g~6.5)	2	23.0	278.1	9.3
(α_i~0)	3	33.0	215.4	18.0
Al_2O_3 (4 minutes)	1	14.0	7.0	5.0
(E_g~6.2)	2	22.8	295.4	9.0
(α_i~0)	3	33	150.2	14.0

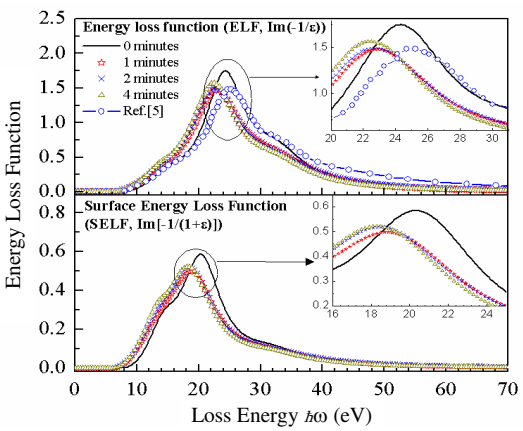

Fig. 3. Energy loss functions (ELF) and surface energy loss function (SELF) of α-Al_2O_3 in this study. These energy loss function described parameters in Table 1, which have been used as input to calculate the λK_{th} values of Fig. 2. We have included the ELF from Ref. [5] for comparison.

The optical properties of α-Al_2O_3 before and after sputtering are shown in Fig. 4-5. They were determined from ELF as a function of electron energy. Figure 4 shows value of reel part (ε_1) and imaginary part (ε_2) of dielectric functions. The variations of ε_1 and ε_2 show the insulating behavior well. As can be seen in the insert figure in Fig. 4, the intensity of the main peak decreases to the lower position for 1 minute sputtering and then increases slightly as the sputtering time increases further.

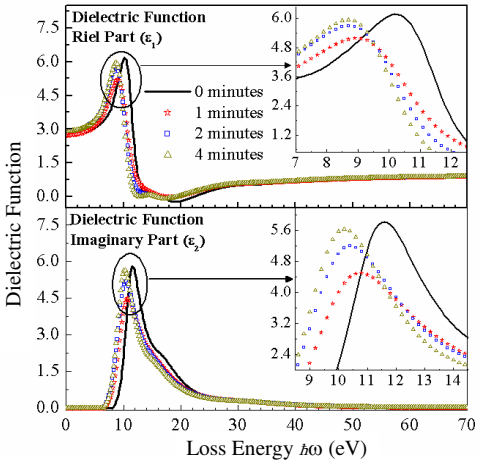

Fig. 4. Real part (ε_1) and imaginary part (ε_2) of dielectric functions of α-Al_2O_3 determined in this study.

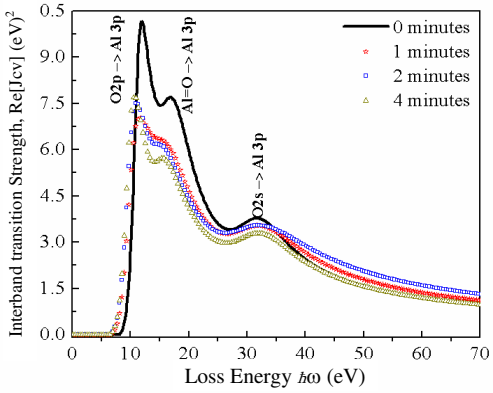

Fig. 5. Real part of Interband transition strength (J_{CV}).

The peak position after sputtering also moves slightly to lower energy loss as the sputtering time increases. The resonance energy of α-Al_2O_3 also changed after sputtering, as indicated by the maximum peak position of imaginary part of dielectric function (ε_2) around ~11-12 eV whereas, at the same position, the real part of dielectric function (ε_1) declines to nearly 0 [22]. The intersection between ε_1 and ε_2 can be observed in the energy region of $\varepsilon_1 \approx \varepsilon_2$; after sputtering, that position also moves to lower energy positions which correspond to the bulk plasmon, which is defined clearly by the peak in the ELF. The shift in bulk plasmon to the lower energy position after sputtering is expected as the oxygen electron concentration decrease in α-Al_2O_3 [1]. The energy loss region above the bulk plasmon peak represents high transparency, as at this energy $\varepsilon_2=k=0$, as we can see clearly in Fig. 6.

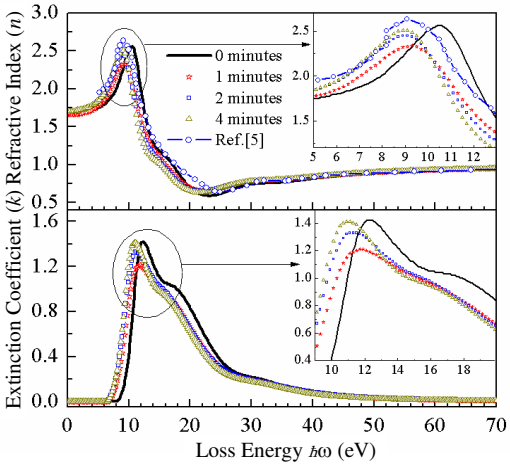

Fig. 6. Index of refractive (n) and extinction coefficient (k) of α-Al_2O_3 determined in this study. We have included index of refractive (n) from Ref. [5] for comparison.

The optical response in terms of interband transition strength spectra, shown in Fig. 5, was developed to describe the features of the electronic structure. Interband transition strength arise from O2p states, from Al=O bonding states and from O2s states [23,24]. The intensity of interband transition strength of of Al_2O_3 decreases as the sputtering times increases; this indicated that the number of O bonding with Al formation decreases in Al_2O_3 film with increasing sputtering times.

Here we render the optical response in terms of the interband transition strength, $J_{CV}(E)$, related to ε(ω) by [23,24]

$$J_{CV}(E) = \frac{m_o^2}{e^2\hbar^2}\frac{E^2}{8\pi^2}\left(\varepsilon_2(E) + i\varepsilon_1(E)\right) \qquad (4)$$

where $J_{CV}(E)$ is proportional to the transition probability and has a unit of g cm^{-3}. For computational convenience we take the prefactor $m_o^2e^{-2}\hbar^{-2}$ in equation above, whose value in cgs units is 8.289×10^{-6} g cm^{-3} eV^{-2}, as unity. Therefore the units of the $J_{CV}(E)$ spectra shown in Fig. 5 are eV^2.

Figure 6 shows value of refractive index (n) and extinction coefficient (k) as function of electron energy. The energy loss region above the bulk plasmon peak represents high transparency, as at this energy $\varepsilon_2=k=0$, as we can see clearly in Fig. 5. The intensity of the main peak in n and k of α-Al_2O_3 decreases after sputtering for 1 minute and then

increases slightly as the sputtering time increases further, as can be seen clearly in the insert figure. The peak position of the main peak also decreases slightly as the sputtering time increases. The peak position and intensity change, which indicates that the optical properties of α-Al_2O_3 change after sputtering. From our results we conclude that the intensities, shapes, and peak positions of the dielectric function (ε_1 and ε_2), refractive index (n) and extinction coefficient (k) are different for α-Al_2O_3 before and after sputtering. These changes are mainly caused by the modification in the O2*p* electron configuration.

CONCLUSION

We obtained and carried out quantitative analysis based on model proposed by Tougaard and Yubero from α-Al_2O_3 before and after sputtering using primary energies of 0.5, 1.0, 1.5 and 2.0 keV. The ELF and SELF for α-Al_2O_3 show intensity and peak position of bulk plasmon change to the lowest energies after sputtering. We conclude that the electronic structure of α-Al_2O_3 changed caused by the decrease in the amount of oxygen in the compound. The bandgap of α-Al_2O_3 slightly decreases from 8.2 eV to 6.39 eV after sputtering due to the change in the stoichiometric form of α-Al_2O_3. The optical properties, e.g., index refractive (n), extinction coefficient (k) and dielectric function (ε) of α-Al_2O_3 after sputtering were obtained from REELS spectra by using QUEELS-ε(k, ω)-REELS software, and was found dependent of sputtering times.

REFERENCES

1. M.A. Vasylyev, S.P. Chenakin and V.A. Tinkov, Vacuum **78** (2005) 19.
2. G.V. Kornich, G. Betz, V. Zaporojtchenko, *et al*., Nucl. Instrum. Methods. Phys. Res. Sec. B **255** (2007) 233.
3. E.C. Rangel, N.M. Dos Santos, J.R.R. Bortoleto, *et al*., Appl. Surf. Sci. **258** (2011) 1854.
4. E.V. Johnson, S. Pouliqsuen, P.A. Delattre, *et al*., J. Non-Cryst. Solids **358** (2012) 1974.
5. R.H. French, H. Mullejans and D.J. Jones, J. Am. Ceram. Soc. **81** (1998) 2549.
6. S. Tougaard and F. Yubero, 2008 QUEELS-ε(k,ω)-REELS: *Software Package for Quantitative Analysis of Electron Energy Loss Spectra; Dielectric Function Determined by Reflection Electron Energy Loss Spectroscopy*. Version 3.02. http://www.quases.com. Retrieved in August (2013).
7. Hajati, O. Romanyuk, J. Zemek, *et al*., Phys. Rev. B **77** (2008) 1.
8. D. Tahir, E.K. Lee, S.K. Oh, *et al*., J. Appl. Phys. **106** (2009) 084108.
9. D. Tahir, E.K. Lee, E.H. Choi, *et al*., J. Phys. D: Appl. Phys. **43** (2010) 255301.
10. O. Romanyuk, P. Jiricek, J. Zemek, *et al*., J. Appl. Phys. **110** (2011) 043507.
11. D. Tahir, H.J. Kang and S. Tougaard, ITB J. Sci. **43A** (2011) 199.
12. D. Tahir, Y.J. Cho, S.K. Oh, *et al*., Surf. Interface Anal. **42** (2010) 1566.
13. D. Tahir, E.K. Lee, S.K. Oh, *et al*., Surf. Interface Anal. **42** (2010) 906**.**
14. D. Tahir and S. Tougaard, J. Appl. Phys. **111** (2012) 054101.
15. D. Tahir and S. Tougaard, J. Phys.: Condens. Matter **24** (2012) 175002.
16. Y.S. Denny, H.C. Shin, S. Seo, S.K. Oh, H.J. Kang, D. Tahir, S. Heo, J.G. Chung, J.C. lee and S. Tougaard, J. Electr. Spect. Rel. Phenom. **185** (2012) 18.
17. H.C. Shin, D. Tahir, S. Seo, *et al*., Surf. Interface Anal. **44** (2012) 623.
18. S. Tougaard and I. Chorkendorff, Phys. Rev. B **35** (1987) 6570.
19. F. Yubero and S. Tougaard, Phys. Rev. B **46** (1992) 2486.
20. F. Yubero, J.M. Sanz, B. Ramskov, *et al*., Phys. Rev. B **53** (1996) 9719.
21. F. Yubero, S. Tougaard and E. Elizalde, *et al*., Surf. Interface Anal. **20** (1993) 719
22. W. Bekhti and M. Ghamnia, Catal. Today **89** (2004) 303.
23. D.J. Jones, R.H. French, H. Mullejans, *et al*., J. Mater. Res. **14** (1999) 4344.
24. S. Loughin, R.H. French, L.K. De Noyer, *et al*., J. Phys. D: Appl. Phys. **29** (1996) 1740.